

# Tunable Multi-Modal Locomotion in Soft Dielectric Elastomer Robots

Mihai Duduta, Florian Berlinger, Radhika Nagpal, David R. Clarke, Robert J. Wood and F. Zeynep Temel

**Abstract**—Soft robots require strong, yet flexible actuators for locomotion and manipulation tasks in unstructured environments. Dielectric elastomer actuators (DEAs) are well suited for these challenges in soft robotics because they operate as compliant capacitors and directly convert electrical energy into mechanical work, thereby allowing for simple design integration at a minimal footprint. In most demonstrations, DEA-based robots are limited to a single mode of locomotion, for example crawling, swimming, or jumping. In this work, we explored a range of actuation patterns in combination with a novel actuator design to enable multi-modal locomotion, whereby an actuation pattern is defined by an actuation voltage (proportional to the applied electric field) and frequency (the actuation rate). We present a DEA robot capable of three different gaits including crawling, hopping, and jumping. In addition, our robot can set itself upright by performing a roll, for example to prepare for the next jump after landing on its side. These results demonstrate that DEAs can be used as versatile experimental devices to validate locomotion models, in both natural and engineered systems.

**Index Terms**—soft robotics, dielectric elastomer actuators, jumping robot, impulsive system, multi-modal locomotion.

## I. INTRODUCTION

**A** KEY area of interest across the field of robotics is making robots more adaptable to their operating environments in order to improve their performance in tasks such as search and rescue, reconnaissance, or manipulation of delicate objects. The goal of having robots that better suit their environments can be achieved in different ways: one approach is to make the robot’s body more compliant, which has led to the emerging field of soft robotics[1], [2], [3]. Another approach is to increase the mobility of the robot, in particular by enabling different modes of locomotion for different types of terrain[4], [5], [6]. Both approaches can

take inspiration from nature, where the majority of animals have evolved with soft bodies and compliant joints[7], and have the ability to transition between modes of locomotion depending on external conditions[8], [9]. A bio-inspired soft robot capable of multi-modal locomotion then becomes a useful device both for complex robotic tasks, as well as for understanding locomotion in the corresponding biological system.

Focusing on multi-modal locomotion in natural systems, we observe that animals take one of two approaches. The first approach is relatively rare and applies to animals which use different appendages and muscles for different types of motions. One example is the black-beard gliding lizard (*Draco melanpogon*) which uses its limbs for crawling, and deploys a patagium for aerial gliding[10]. The same principle of employing different appendages and muscles for different motions has been used in engineered systems: the Dash crawler[11] was modified with a jumping module to allow it to overcome large obstacles[12]. However, this approach increases the complexity of the robot, since different actuators are needed for each mode of locomotion.

A second approach is observed in natural systems much more often, and relies on using of the same appendages and muscles for different modes of locomotion. The common cockroach is capable of rapidly transitioning between walking, running, climbing, and wedging[13], while salamanders can move effectively in both water and on land [14]. In both cases, the bio-inspired robots made to reproduce these behaviors become useful tools for experimental validation of locomotion models[15], [16]. The other advantage of this second approach is a simpler robot design and construction, since the same components are used for different modes of locomotion.

Compared to these relatively complex animals and robots, simpler examples of multi-modal locomotion can be found in soft-bodied insect larvae and caterpillars. These organisms typically have long slender bodies which can bend to produce a range of motions, including crawling, jumping, and rolling[17]. Larvae examples include legless fruit fly larvae (*Ceratitis capitata*)[18], the soft bodied larvae of the piophilid fly (*Prochyliza xanthostoma*)[19], as well as the worm-like larvae of the gall midge (*Asphondylia* sp.)[20].

For soft robots, there are limited choices for actuators, constraining the capabilities for multi-modal locomotion, and reducing the ability to build experimental tools to validate theoretical models of locomotion. Still, several examples have shown the versatility of soft bodies capable of different modes of locomotion. One recent example uses composites of

Manuscript received: October, 14, 2019, Revised: February, 5, 2020, Accepted: March, 4, 2020.

This paper was recommended for publication by Editor Cecilia Laschi upon evaluation of the Associate Editor and Reviewers’ comments

The research was supported by the National Science Foundation (Materials Research Science and Engineering Center, award no. DMR14-20570), the Army Research Office (award no. W911NF-15-1-0358), and the Wyss Institute for Biologically Inspired Engineering. Any opinions, findings, and conclusions or recommendations expressed in this material are those of the authors and do not necessarily reflect the views of the National Science Foundation.

The authors are with the John A. Paulson School of Engineering and Applied Science at Harvard University, Cambridge, Massachusetts, USA. Florian Berlinger, Mihai Duduta, Robert Wood, F.Z. Temel and Radhika Nagpal are also with the Wyss Institute for Biologically Inspired Engineering, Boston, Massachusetts, USA. F.Z. Temel is also with the Robotics Institute, Carnegie Mellon University, Pittsburgh, PA, USA. E-mail: mduduta@g.harvard.edu, ztemel@andrew.cmu.edu

Digital Object Identifier (DOI): see top of this page.

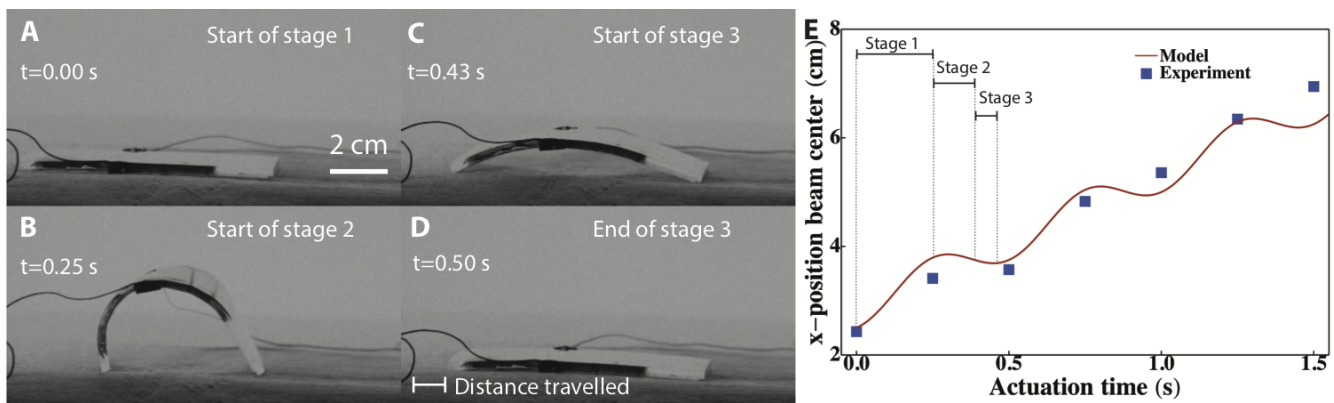


Fig. 1. **A-D.** Example of an actuation cycle which allows the robot to crawl to the right. **E** Comparison between modeled and experimental position of the DEA robot's center of mass over three cycles at 4 Hz. The three stages of crawling are indicated with dashed lines.

elastomers and magnetic microparticles to make inchworms that respond to applied magnetic fields[21]. The resulting soft robots show great versatility by swimming, jumping, rolling, and climbing, but require large magnetic fields which reduces their applicability for operation in unstructured environments. A different approach uses shape memory alloy coils to power a robotic replica of a caterpillar capable of inchworm crawling and ballistic rolling[6]. These compelling examples have some inherent limitations in both terms of scale and need for specific operation parameters, such as magnetic fields.

Overcoming limitations, such as the need for external magnetic fields, is possible by using dielectric elastomer actuators (DEAs) to power soft robots. DEAs are compliant capacitors[22], that operate as soft electro-mechanical transducers and convert electrical energy into mechanical work. Different designs of DEA-powered robots have already accomplished different modes of locomotion, such as crawling and hopping[23], autonomous swimming[24], and flapping wing flight[25]. Multilayer DEAs made from strain-stiffening elastomers and carbon nanotubes actuate without the need for pre-stretch[26], and have been demonstrated in fast crawling inchworm robots[27]. More recent advances have shown operation at high frequencies ( $>200$  Hz)[28], as well as specific energies on par with natural muscle (20 J/kg)[29]. These high energy density actuators have been used to demonstrate impulsive motions in cantilever beams, where rapid shape changes can be converted into jumping motions[30].

The objective of this work was to develop a unified framework to understand how dielectric elastomer actuators can be designed and powered to demonstrate multi-modal locomotion. We started by developing a model for crawling in a bending beam driven by an applied periodic voltage. Past modeling work on bending beams was extrapolated to give guidance for ranges of applied voltage and actuation period that correspond to different modes of locomotion. We built and tested bending robots capable of jumping from a curved starting configuration, and showed the same robots to be capable of crawling and hopping. In addition, we found a

new gait useful for self-righting and high speed locomotion: rolling.

We also experimented with a novel design version, in which the DEA robot starts in a resting flat configuration. By adding an inactive segment we achieved directional jumping, useful for overcoming obstacles. Lastly we organized our results in a behavior diagram, linking the applied period of deformation (or actuation frequency) to the applied maximum voltage (or maximum strain), to show that both robot configurations exhibit the same locomotion modes, under similar conditions.

## II. MATERIALS AND METHODS

### A. Actuator Fabrication

We developed a model for periodic actuation, and used it to select the elastomer and strain limiting materials. To minimize the number of trials, we focused this study on bending beam DEAs, 5 cm long, 2 cm wide, 1 mm thick, weighing 0.9 grams.

We used established methods [26], [27] to fabricate multilayer actuators by sequential stacking of elastomers and electrode layers. The elastomer layer was produced by spin coating of a viscous oligomer (CN9018 from Sartomer, Exton, PA) with 7.5% 1,6-hexanediol diacrylate (Sigma Aldrich, St. Louis, MO) at 3000 RPM for 30 seconds (Laurell Technologies), then UV curing for 120 seconds under 395 nm light, yielding a layer of thickness  $48 \pm 3 \mu\text{m}$ . The electrodes were ultrathin mats of carbon nanotubes (from Nano-C, Westwood, MA), stamped directly onto the elastomer through a pre-cut mask. A schematic of the stamping process is given in Supplemental Figure S3. The adhesion of a stiffer substrate (Mylar, 75 microns thick) caused the two material: DEA + Mylar composite to preferentially bend when actuated. All the power electrodes in the multilayer were connected to each other by cutting through the stack, applying colloidal silver paste, and attaching leads with conductive carbon tape. The same process was repeated for the ground electrodes, respectively.

Two types of actuators were made: the first in which the resting state of the DEA robot was curved, and the second in

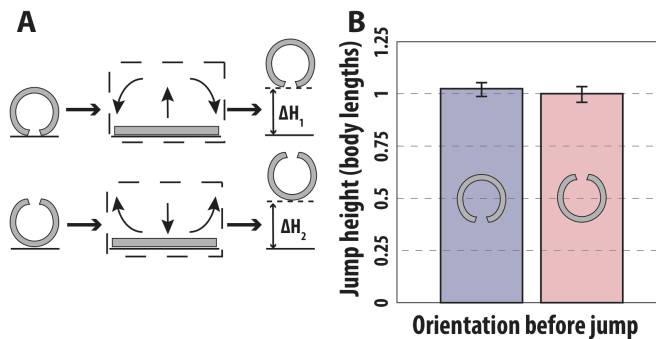


Fig. 2. Comparison of two energy-equivalent ways of jumping with curved DEA robots: **A** A robot can either push with its ends (top) or with its middle (bottom) into the ground. **B** The corresponding heights for both ways of jumping are almost identical, suggesting that jumping height depends predominantly on the total energy stored in the system. Heights were obtained with three robots of each type, whereby each robot’s jump height was measured in five different experiments.

which the resting state was flat, a novel design for a jumping DEA robot. To achieve the curved state, the DEA was pre-stretched before adhesion to the Mylar. The resting shape was predicted using earlier work[30]. The chosen shape was cylindrical, as a beam bending out of plane, and was achieved by careful selection of the DEA and Mylar thicknesses (1 mm and 75 microns, respectively). A schematic of the bonding with the strain limiting layer is given in Supplemental Figure S4. For both the curved and flat starting states, the predicted strain at the maximum voltage of 6 kV was 15% relative to initial length. Accordingly, the pre-strain was selected to match the expected 15% strain, to ensure a flat shape when charged.

### B. DEA Characterization

The main goal of this work was to establish the ranges of frequency and actuation voltage under which a specific mode of locomotion is observed. To that end, we powered the DEA robots using a Trek high voltage power supply (610E). The range of voltages applied was 2.5-7 kV, corresponding to electric fields in the 50-140 V/ $\mu\text{m}$  range for 50 micron layers. Higher voltages caused dielectric breakdown, while lower voltages did not produce sufficient deformation to allow for locomotion.

The frequency of the applied high voltage was controlled with a Rigol waveform generator. The range of frequencies was between 1 and 100 Hz, applied as square or sinusoidal waves. Lower frequencies than 1 Hz allowed the actuators to crawl, but at a very slow ground speed. Frequencies greater than 100 Hz did not cause appreciable deformation because of the relatively large viscoelastic losses in the elastomer. For crawling, hopping, and rolling demonstrations, the deformation profile was symmetric as a function of time (Supplemental Figure S5A). For jumping demonstrations we found that symmetric profiles caused damage to the robot, due to high current spikes during charging, as well as inconsistent mechanical deformation. By comparison, an asymmetric profile of slowly charging the actuator, and

rapidly discharging led to improved jump reliability (Supplemental Figure S5B). All of the jumping examples in this work used asymmetric charge / discharge profiles. Moreover, the discharge period was used to calculate the actuation frequency used to compare the locomotion modes in Figure 7.

The motion was recorded using a high speed camera (Phantom v7.3 from Vision Research, Wayne, NJ). The images were captured at 120 frames per second, and a resolution of  $800 \times 600$  pixels. The images were processed to record jump heights, as well as ground speed. We note that all of these actuators were tested without using appendages which are known to improve friction and increase ground speed[31]. The speeds and heights were used primarily to compare relative performance between the multilayer DEAs described in this work.

## III. RESULTS

### A. Model of Periodic Actuation

A model of beam deformation had been developed independently[32] to explain how adding stronger friction at one end of a bending beam compared to the other end causes forward locomotion. In that example, actuation was driven by periodic heating of a two-material cantilever. Following that example, we derived a model of deformation in a two-material laminate, in which one layer is the dielectric elastomer actuator, and the second layer is a strain limiting stiffer material. For simplicity, the model started with the actuator in the flat configuration at rest, and is curved when charged. The full model (in Supplemental Information) links the applied voltage and actuation period to the position of the center of mass of the robot in three key stages:

- **Stage 1:** During charging, the robot curls and the front foot does not slip. Center of mass moves forward.
- **Stage 2:** During discharging, the robot returns to a flat state while the both ends slips. Center of mass moves backwards.
- **Stage 3:** friction at the front foot prevents forward movement, the robot returns to the starting state. Center of mass moves backwards.

Our model described the dielectric elastomer as subjected to periodic actuation by a voltage:

$$V(t) = \begin{cases} V_{max} \times \left( \frac{t}{P} \right) & , 0 < t < P \\ V_{max} \times \left( 2 - \frac{t}{P} \right) & , P \leq t < 2P \end{cases} \quad (1)$$

where  $V_{max}$  is the maximum voltage applied, and  $P$  is the period of actuation. The curvature of the cantilever beam can be determined from the material and geometric properties of the elastomer and stiffening layer, assuming the beam is free to deform only along its length:

$$\kappa = - \frac{6j(1+n)\epsilon_0\epsilon}{2E_e t_s^3 (j^2 n^4 + 4jn^3 + 6jn^2 + 4jn + 1)n} V^2 \quad (2)$$

where  $\epsilon_0$  is the permittivity of free space,  $\epsilon$  is the dielectric constant of the elastomer,  $E_e$  is the Young’s modulus of

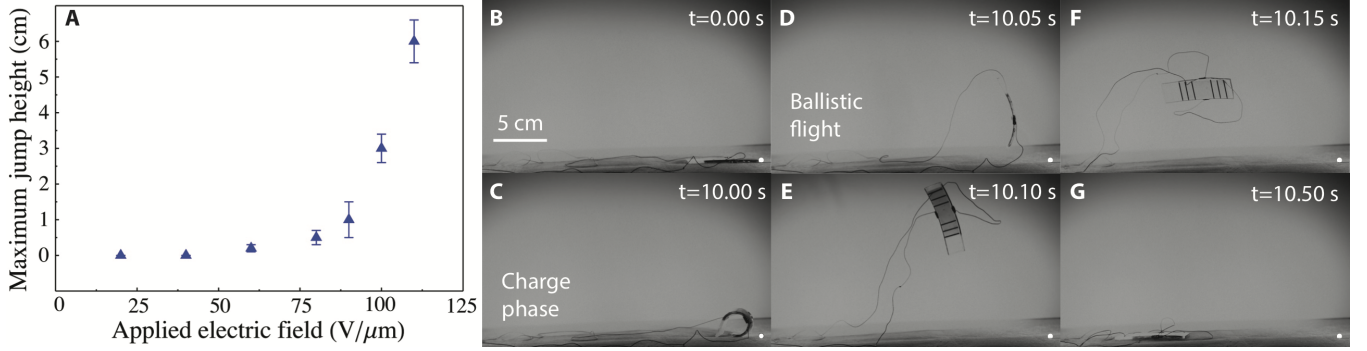


Fig. 3. Jumping behavior of flat DEA robots: **A** The jump height depends non-linearly on the applied electric field, with higher jumps being possible at higher applied fields. **B-G** Stages throughout the jump of a DEA robot starting in a flat configuration. A white dot is used on the bottom right of each panel to indicate the starting position of the composite. When charged (**C**) the robot makes use of an inactive foot at the end of the body to have an orientation that leans onto the ground. From this orientation, when energy is released, the composite undergoes ballistic flight (**D,E,F**).

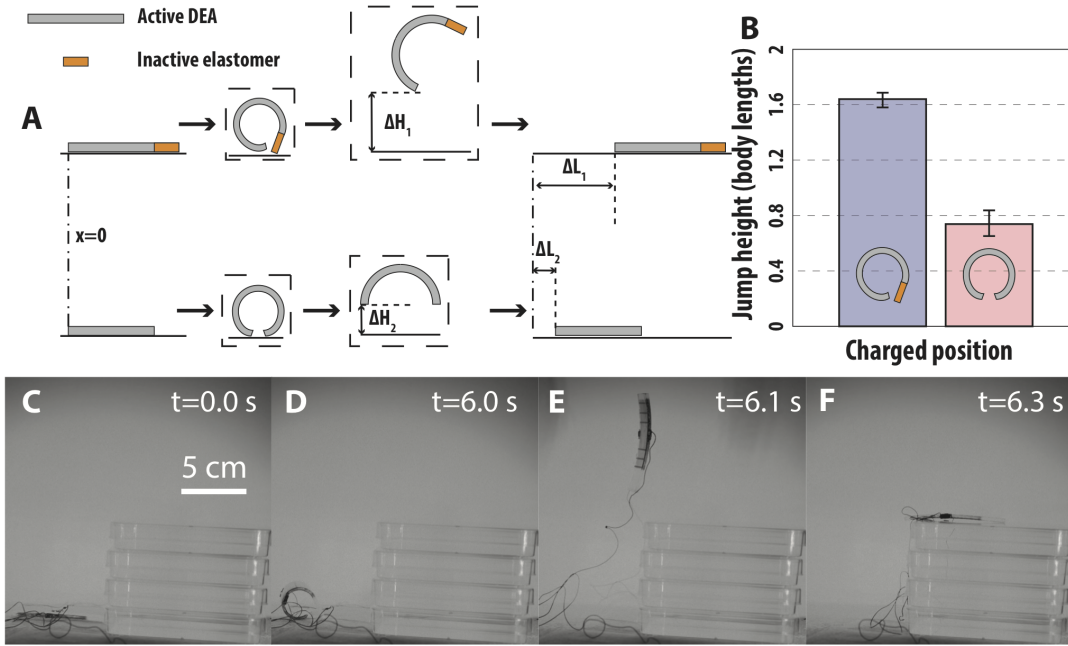


Fig. 4. Jumping over obstacles: **A** The slight difference in body orientation enabled by a passive foot allows the asymmetric DEA to jump higher, further, and more target oriented than a symmetric DEA (**B**). **C-F** The doubling in jump height, as well as control over jump direction, allows the asymmetric DEA to jump onto an obstacle roughly as tall as its body length (6 cm) formed by stacking four square plastic petri dishes.

the elastomer,  $t_s$  is the thickness of the stiffening layer,  $j = E_e/E_s$ , where  $E_s$  is the Young's modulus of the stiffening layer,  $n = t_e/t_s$ , where  $t_e$  is the thickness of the elastomer. From the curvature and periodic voltage, we derived a formula for the position of the center of mass along the x-axis, as a function of the deformation period and voltage. The formula is applicable to the first stage of deformation, as the actuator is charged and the friction at the front end keeps that point fixed:

$$x_{C1} = \frac{L}{2} - \frac{\sin\left(\frac{\beta L V_{max}^2}{2} \left(\frac{t}{p}\right)^2\right)}{\beta V_{max}^2 \left(\frac{t}{p}\right)^2} \quad (3)$$

where  $\beta$  is a constant term that incorporates material and

geometric properties, while  $L$  is the length of the cantilever beam along which deformation occurs.

The two other stages of movement occurred as the beam returns to the flat position, during discharge of the actuator. The details are shown in the Supplemental Information, while corresponding states for actuators studied in this work are shown in Figure 1 (A through D). The model was used to compare the position of the actuator's center of mass with observed locomotion of a crawling beam at 4 Hz, as shown in Figure 1E. The results indicated the model captured the observed motion relatively well, with two limitations: the modeled beam is symmetric, while the experimental beam has an inactive front component, which helps in other modes of deformation. In addition, the friction at either end of the experimental beam is not carefully controlled, which leads

to slipping and deviation between experimental and modeled results. Overall, the model we developed linked the two key actuation parameters (maximum applied voltage  $V_{max}$ , and actuation period  $P$ ) with displacement of the center of mass, and can be developed further to describe acceleration of the actuator.

The cited bending beam model[32] has already been expanded[33] to show simple bending beams can exhibit multiple modes of locomotion, by modulating the applied strain and deformation period. We found a direct correspondence to dielectric elastomer actuators, and our current model: the strain is directly proportional to the Maxwell stress, which depends on the square of the applied electric field. Similarly, the deformation rate corresponds to the actuation frequency of the robot. Without aiming to duplicate existing work, we used the framework of the expanded model, as well as our own, to determine the ranges in applied voltage and frequency that control different modes of locomotion.

### B. Locomotion Modes

By modulation of the actuation voltage and frequency, we achieved four modes of locomotion:

- **Crawling** occurred when the robot (or animal) moves forward by lengthening and shortening the distance between the points at which it makes contact with the ground. Forward locomotion was due to a friction coefficient that is lower in the forward direction than in the backward direction.
- **Hopping**, by comparison, occurred at a higher rate of deformation and was characterized by the entire robot losing contact with the ground briefly.
- **Jumping** was an impulsive movement, in which the ground forces and specific power were higher than in hopping with the goal of maximizing the airborne phase[34].
- **Rolling** was the mode in which the robot takes a curved shape that allowed it to roll relative to the ground[6].

By evaluating the behavior in a quantitative manner, we described a phase diagram (Figure 7) which captured the entire spectrum of behaviors, as a function of the applied voltage and actuation frequency.

### C. Jumping Demonstrations

We have demonstrated jumping with a curved-beam DEA robot previously[30]. Here we conducted a more rigorous performance analysis to achieve increased jumping heights. In addition, we designed a novel DEA robot version, which starts jumping from a flat configuration. The design allowed for the addition of a performance-enhancing passive foot, which increased jump height and gave directional control.

Jumping of a DEA robot used an electric latch to release mechanical energy stored in a DEA robot. By rapidly discharging the DEA, the Maxwell stress applied to keep the elastomer stretched is removed. The discharged DEA aimed to return to its original curved shape, and could push into

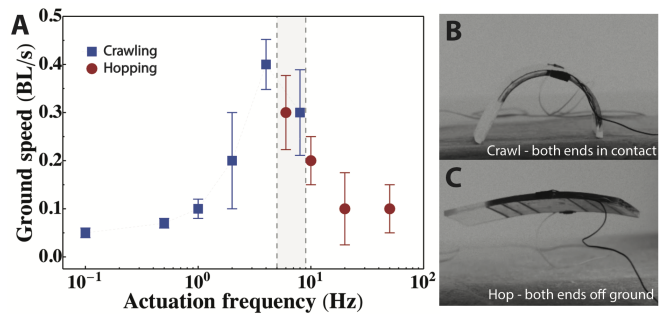


Fig. 5. Transition from crawling to hopping: **A** Speeds for ground-based locomotion peaked at around 0.38 BL/s at an actuation frequency of 7 Hz, at the transition from crawling to hopping. Speeds for pure crawling at low frequencies, and pure hopping at high frequencies were similar, and about a third of the maximum speed. Data from one DEA robot tested at multiple frequencies, three times each, all at 5 kV. The shaded central region shows the transition from crawling to hopping which depends on how the actuator is operated. **B** Example of a crawl, with at least one end in contact with the ground. **C** Example of a hop, with both ends disconnected from the ground.

the ground either with its ends or its center, depending on the orientation (Figure 2). This behavior is also presented in Supplemental Video S1. The robot orientation where the ends point at the ground at rest delivered a jump height of  $5.8 \pm 0.2$  cm, for a total jump duration of 0.2 s, with very little distance traveled relative to the starting position ( $< 2$  cm). The robot orientation where the ends point upwards at rest delivered a jump height of  $5.6 \pm 0.3$  cm, for a total jump duration of 0.2 s, similarly with a small displacement relative to the initial position. Surprisingly, there was little difference in jump heights depending on how the DEA is oriented relative to the ground. This finding suggested that the main driver for jump height is the total energy stored in the system, which is equal between the two modes of jumping. Additionally, we expect friction with the ground to play a negligible role in how energy is released, given the jumps achieved in the first orientation where the ends push into the ground.

Existing models[33] predicted that bending beam actuators can also jump from a flat starting configuration. The flat DEA robot was made similarly to the robot described in Fig. 2, without pre-stretching the elastomer before attaching the Mylar. During this experiment the charge time was higher than the discharge time, to allow the body to form a loop such that the energy release is effective at causing a jump, as shown previously in natural systems[20]. For slow charging rates, the input electrical energy depended on the square of the applied electric field, therefore the stored mechanical energy should depend non-linearly on the applied electric field, given some electro-mechanical efficiency of the system.

Higher jumps were observed at higher applied fields (Fig. 3A). For the longest jump recorded, the maximum height for the center of mass was 8.7 cm, while the robot traveled 6.7 cm relative to its initial starting point. The time between takeoff and landing was 0.3 seconds, resulting in a ground speed during the jump of 22.3 cm/s. We calculated the cost of transport (CoT: energy used normalized by distance

traveled, weight of the robot, and acceleration due to gravity) following an established approach for jumping robots[35] and find the value to be 29.6. This value was on the same order of magnitude with other jumping robots (7-13 for a 7 gram jumping robot[35], depending on take-off angle), and natural systems (8-80 for jumping larvae[20], which are nearly two orders of magnitude lighter). Improving the electro-mechanical efficiency of the DEAs (for example, from 1% to 20% as observed in natural systems[36]) is needed to power jumping systems with greater on-board capabilities (e.g., power autonomy and control).

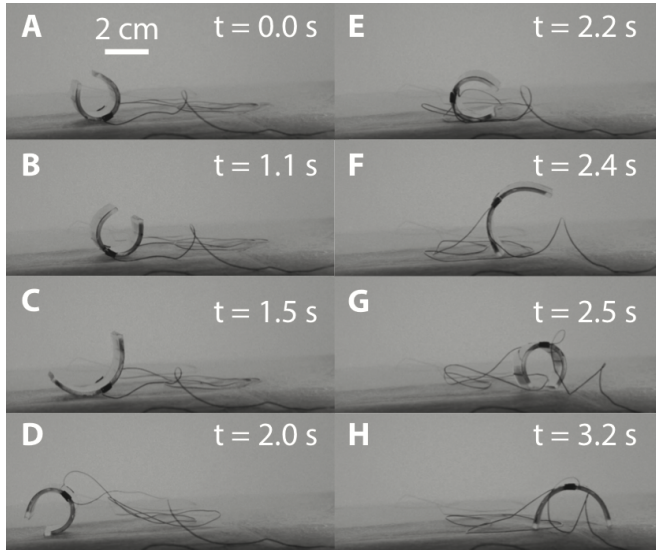


Fig. 6. Rolling behavior of curved DEA composites: **A** Starting position with ends pointing upwards. **B-F** Frames from motion along the way as the actuated DEA swings from one side to the other. **G** Rolling is successful, ends are pointing down. **H** At the same frequency but different orientation, the DEA crawls.

In flat jumping DEA robots, the addition of a passive foot helped orient the body in such a way as to push more effectively against the ground to jump higher and further (Figure 3 and Supplemental Video S1). This modification was supported by finite element modeling (FEM) of simple bending beams deforming at high rates[33]. The control over jump height and direction was used to overcome obstacles (Figure 4). The results in Fig. 4B show that there was a clear advantage to having a passive foot that directs some of the energy into the ground to allow for ballistic flight. This result is not surprising, considering that in the resting state the DEA robot is flat, so ground forces would be minimal. The addition of the passive foot allowed the DEA robot to jump onto obstacles that are taller than its body length (6 cm). The ability to overcome obstacles is also shown in Supplemental Video S1.

#### D. Crawling and Hopping Demonstrations

Bending beam DEAs have shown the ability to crawl[37] at relatively high speeds, as fast as one body length (BL) per second[27]. In this work we considered crawling to be a linear motion in which at least one end of the DEA is in

contact with the ground at all times. By comparison, hopping can occur when there is sufficient power in the system for the DEA to completely lose contact with the ground. To distinguish from jumping, hopping is displacement limited, with small steps less than 0.5 BLs each. Intuitively, hopping was expected to occur at higher frequencies than crawling[38], and at lower voltages than jumping. In practice, we observed regions of overlap between the different locomotion modes. We did not control the relative friction between the robot and the ground, therefore slight changes in orientation and ground contact may be responsible for the range of behaviors in the transition phase.

The transition from crawling to hopping depended heavily on how the actuator is powered (Figure 5). For the example in the figure, each test corresponded to actuation directly from resting at the target frequency. However, we observed that during frequency sweeps from 1 Hz towards 100 Hz, crawling was occasionally observed at frequencies where hopping would occur if powered directly from a rest state, likely due to a dynamic effect. The range in which crawling and hopping behavior are both observed is shaded in the figure. Examples of both gaits are shown in Supplemental Video S1. Crawling from a flat starting state is shown in these examples, but similar behavior is observed for DEAs which start in a curved state. The highest observed crawling ground speed was 2 cm/s, while the robot was driven at 4 Hz, leading to a CoT of 113.4. The highest observed hopping ground speed was 1.5 cm/s, while the robot was driven at 7 Hz, leading to a CoT of 148.1. These values are higher than the CoT for jumping because the robot does not have additional elements to improve directional friction and slides relative to the ground. The same type of increase in CoT is observed in living systems, for example the gall-midge larvae have CoT in the 8-80 range for jumping, and CoT higher than 2300 for crawling[20].

#### E. Rolling Demonstration

Rolling is a mode of locomotion observed in natural and engineered systems for both rapid movement[6], and self-righting[39]. Using previous modeling work as inspiration[33], the beam was made to have an almost circular shape to roll without interruption. For the DEAs in this work, rolling was applicable only to composites which have a curved resting state. Specifically, the level of pre-strain was increased to 25% to cause an almost circular resting shape (opposed to the half circle in jumping and crawling examples). Similar to a swinging pendulum, the rolling DEA needed to be driven close to its resonant frequency to maximize side to side displacement. Under the right conditions, we expected the beam to be at moving towards one end with some velocity, then come to rest in its fully curved state. At that point the beam's momentum was expected to push the center of the beam over one end. As the actuator was re-charged, the beam would flatten, and maintain the inverted orientation. For such a DEA oriented with its ends upwards, rolling could be used as a self-righting mechanism. Once the DEA rolled onto a position where the ends point down, it could continue to crawl.

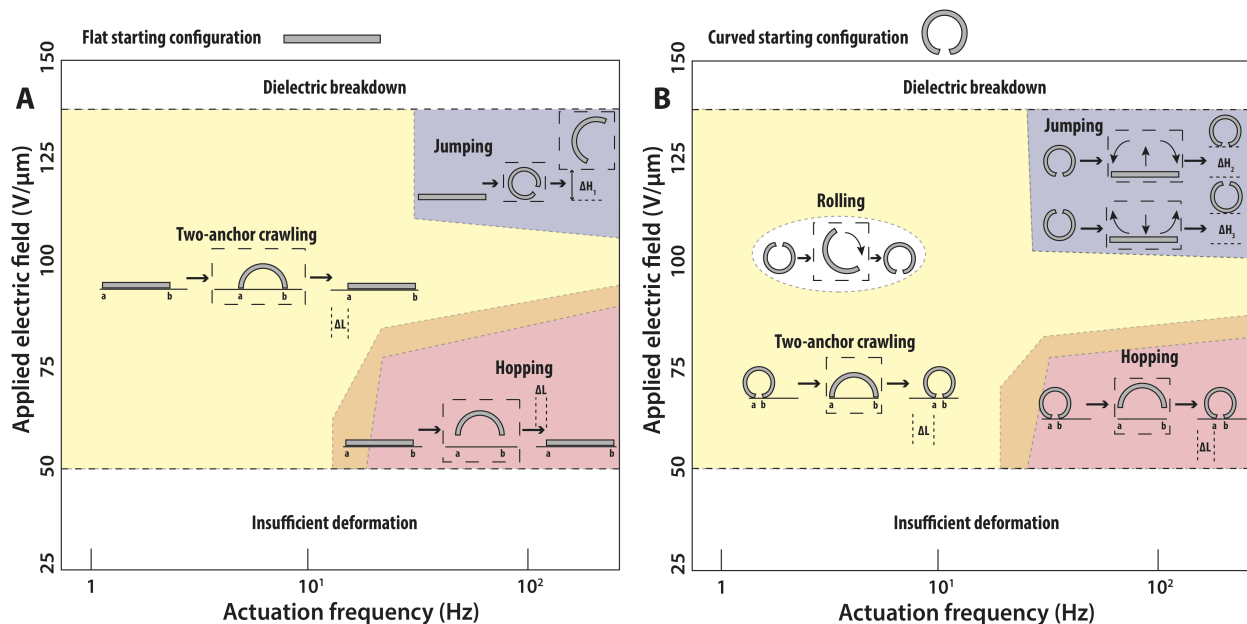


Fig. 7. Locomotion modes as a function of applied field and actuation frequency determined experimentally: **A** Left panel shows the modes of behaviors observed in a novel DEA composite starting in a flat configuration. Most of the space consists of crawling behavior (yellow background) at all ranges of applied fields, below 20 Hz. At higher frequencies, for rapid release of energy stored at high fields, DEAs are able to jump (blue background). When small fields are applied at high frequencies, the DEAs are able to hop (red background). The region with overlap between hopping and crawling behavior is depicted as shaded orange. **B** Right panels shows the same trends and the same color coding for a DEA starting in a curved configuration. The white area in the center of the figure shows the range of applied field and frequency under which rolling can be used to self-right the DEA robot.

For the example in Figure 6, the rolling occurred after 3-5 seconds of actuation at 4 Hz and 3.5 kV, the resonant frequency of the composite (also shown in Supplemental Video S1). Actuation at higher frequencies led to vibration of the ends pointing up, but no significant movement of the DEA robot center. Similarly, actuation at lower frequencies moved the ends in and out, but did not cause movement of the center. For the example shown, the maximum distance travelled as part of the roll was 3.2 cm, in a 0.5 second span, leading to a CoT of 35.4. In this work, rolling was limited as a subset of crawling, used for self-righting. However, we expect that a more careful study of actuation and rest patterns, in an untethered robot[40], can be used for ballistic rolling in which the DEA changes its orientation actively, then rolls in a passive fashion.

#### IV. DISCUSSION

The range of locomotion modes is summarized in an experimental phase diagram, as shown in Figure 7. The behavior exhibited by the robots matches well with the predicted deformation modes from existing models. Deformation is linked to changes in curvature, and any relative changes greater than two orders of magnitude are considered large: *e.g.*, a curved robot with a radius of 1 cm transitioning to a flat state approximated as a 100 cm radius corresponds to a two order of magnitude transition. Similarly, deformation rates larger than the natural frequency of the beam (approximated to be 4 Hz, from [30]) are considered to

be large. For the entire range of applied voltages, at lower frequencies only crawling was observed, in both curved and flat configurations. However, once the rate of energy input increases, a richer set of behaviors emerges. At low fields, where the displacement of the bending beam was limited, the rapid changes in body shape led to hopping. This locomotion can easily become unstable, especially at frequencies higher than 50 Hz, causing the robot to fall to its side which requires a self righting step. If both the energy input (sufficient to cause a change in curvature of two orders of magnitude), and the rate of deformation are high (larger than the natural frequency of the beam), jumping was observed in all body configurations. This mode of locomotion can be particularly useful for overcoming obstacles, as shown by a flat DEA with a passive foot. Lastly, the body shape and large deformations at resonance allowed a curved DEA to show self-righting rolling as another unique mode of locomotion.

The costs of transport for the four modes of locomotion spanned from 29.6 to 148.1, and were comparable to CoTs of insects of similar size[41]. For now, we identify jumping as the more energy efficient locomotion with a CoT of 29.6, as the geometry allows the robot to direct most of the energy into the ground, following the expected trend from natural systems. We expect the CoT to decrease for the other locomotion modes, provided directional friction elements are added to improve contact with the ground, as we have shown earlier[27]. Our experiments demonstrate the versatility of these multi-modal DEAs. The ability to

select from a variety of locomotion modes combined with the compact and simple monolithic design is highly attractive for a variety of applications such as navigating complex and unstructured terrain. More importantly, these simple DEA robots are the first experimental validation of models for soft body deformation leading to different modes of locomotion in biological systems. The results make DEAs capable of rapid deformation an interesting tool for both robot design and the study of natural systems.

## REFERENCES

- [1] C. Majidi, "Soft robotics: a perspective—current trends and prospects for the future," *Soft Robotics*, vol. 1, no. 1, pp. 5–11, 2014.
- [2] D. Rus and M. T. Tolley, "Design, fabrication and control of soft robots," *Nature*, vol. 521, no. 7553, p. 467, 2015.
- [3] S. Kim, C. Laschi, and B. Trimmer, "Soft robotics: a bioinspired evolution in robotics," *Trends in biotechnology*, vol. 31, no. 5, pp. 287–294, 2013.
- [4] L. Daler, S. Mintchev, C. Stefanini, and D. Floreano, "A bioinspired multi-modal flying and walking robot," *Bioinspiration & biomimetics*, vol. 10, no. 1, p. 016005, 2015.
- [5] J. Yu, R. Ding, Q. Yang, M. Tan, W. Wang, and J. Zhang, "On a bio-inspired amphibious robot capable of multimodal motion," *IEEE/ASME Transactions On Mechatronics*, vol. 17, no. 5, pp. 847–856, 2012.
- [6] H.-T. Lin, G. G. Leisk, and B. Trimmer, "Goqbot: a caterpillar-inspired soft-bodied rolling robot," *Bioinspiration & biomimetics*, vol. 6, no. 2, p. 026007, 2011.
- [7] M. Calisti, G. Picardi, and C. Laschi, "Fundamentals of soft robot locomotion," *Journal of The Royal Society Interface*, vol. 14, no. 130, p. 20170101, 2017.
- [8] R. Lock, S. Burgess, and R. Vaidyanathan, "Multi-modal locomotion: from animal to application," *Bioinspiration & biomimetics*, vol. 9, no. 1, p. 011001, 2013.
- [9] S. Patek, J. Baio, B. Fisher, and A. Suarez, "Multifunctionality and mechanical origins: ballistic jaw propulsion in trap-jaw ants," *Proceedings of the National Academy of Sciences*, vol. 103, no. 34, pp. 12787–12792, 2006.
- [10] R. Shine, S. Keogh, P. Doughty, and H. Giragossyan, "Costs of reproduction and the evolution of sexual dimorphism in a 'flying lizard' draco melanopogon (agamidae)," *Journal of Zoology*, vol. 246, no. 2, pp. 203–213, 1998.
- [11] P. Birkmeyer, K. Peterson, and R. S. Fearing, "Dash: A dynamic 16g hexapedal robot," in *2009 IEEE/RSJ International Conference on Intelligent Robots and Systems*. IEEE, 2009, pp. 2683–2689.
- [12] G.-P. Jung, C. S. Casarez, S.-P. Jung, R. S. Fearing, and K.-J. Cho, "An integrated jumping-crawling robot using height-adjustable jumping module," in *2016 IEEE International Conference on Robotics and Automation (ICRA)*. IEEE, 2016, pp. 4680–4685.
- [13] C. F. HERREID, R. J. FULL, and D. A. PRAWEL, "Energetics of cockroach locomotion," *Journal of Experimental Biology*, vol. 94, no. 1, pp. 189–202, 1981.
- [14] A. J. Ijspeert, "A connectionist central pattern generator for the aquatic and terrestrial gaits of a simulated salamander," *Biological cybernetics*, vol. 84, no. 5, pp. 331–348, 2001.
- [15] K. Jayaram and R. J. Full, "Cockroaches traverse crevices, crawl rapidly in confined spaces, and inspire a soft, legged robot," *Proceedings of the National Academy of Sciences*, vol. 113, no. 8, pp. E950–E957, 2016.
- [16] A. J. Ijspeert, A. Crespi, D. Ryczko, and J.-M. Cabelguen, "From swimming to walking with a salamander robot driven by a spinal cord model," *Science*, vol. 315, no. 5817, pp. 1416–1420, 2007.
- [17] J. Brackenburg, "Fast locomotion in caterpillars," *Journal of insect physiology*, vol. 45, no. 6, pp. 525–533, 1999.
- [18] D. P. Maitland, "Locomotion by jumping in the mediterranean fruit-fly larva *ceratitis capitata*," *Nature*, vol. 355, no. 6356, p. 159, 1992.
- [19] R. Bonduriansky, "Leaping behaviour and responses to moisture and sound in larvae of piophilid carrion flies," *The Canadian Entomologist*, vol. 134, no. 5, pp. 647–656, 2002.
- [20] G. Farley, M. Wise, J. Harrison, G. Sutton, C. Kuo, and S. Patek, "Adhesive latching and legless leaping in small, worm-like insect larvae," *Journal of Experimental Biology*, vol. 222, no. 15, p. jeb201129, 2019.
- [21] W. Hu, G. Z. Lum, M. Mastrangeli, and M. Sitti, "Small-scale soft-bodied robot with multimodal locomotion," *Nature*, vol. 554, no. 7690, p. 81, 2018.
- [22] S. Rosset and H. R. Shea, "Flexible and stretchable electrodes for dielectric elastomer actuators," *Applied Physics A*, vol. 110, no. 2, pp. 281–307, 2013.
- [23] J. Zhao, J. Zhang, D. McCoul, Z. Hao, S. Wang, X. Wang, B. Huang, and L. Sun, "Soft and fast hopping–running robot with speed of six times its body length per second," *Soft robotics*, vol. 6, no. 6, pp. 713–721, 2019.
- [24] F. Berlinger, M. Duduta, H. Gloria, D. Clarke, R. Nagpal, and R. Wood, "A modular dielectric elastomer actuator to drive miniature autonomous underwater vehicles," in *2018 IEEE International Conference on Robotics and Automation (ICRA)*. IEEE, 2018, pp. 3429–3435.
- [25] Y. Chen, H. Zhao, J. Mao, P. Chirarattananon, E. F. Helbling, N.-s. P. Hyun, D. R. Clarke, and R. J. Wood, "Controlled flight of a microbot powered by soft artificial muscles," *Nature*, vol. 575, no. 7782, pp. 324–329, 2019.
- [26] M. Duduta, R. J. Wood, and D. R. Clarke, "Multilayer dielectric elastomers for fast, programmable actuation without prestretch," *Advanced Materials*, vol. 28, no. 36, pp. 8058–8063, 2016.
- [27] M. Duduta, D. R. Clarke, and R. J. Wood, "A high speed soft robot based on dielectric elastomer actuators," in *Robotics and Automation (ICRA), 2017 IEEE International Conference on*. IEEE, 2017, pp. 4346–4351.
- [28] H. Zhao, A. M. Hussain, M. Duduta, D. M. Vogt, R. J. Wood, and D. R. Clarke, "Compact dielectric elastomer linear actuators," *Advanced Functional Materials*, vol. 28, no. 42, p. 1804328, 2018.
- [29] M. Duduta, E. Hajjesmaili, H. Zhao, R. J. Wood, and D. R. Clarke, "Realizing the potential of dielectric elastomer artificial muscles," *Proceedings of the National Academy of Sciences*, p. 201815053, 2019.
- [30] M. Duduta, F. Berlinger, R. Nagpal, D. Clarke, R. Wood, and F. Z. Temel, "Electrically-latched compliant jumping mechanism based on a dielectric elastomer actuator," *Smart Materials and Structures*, vol. 28, no. 9, p. 09LT01, 2019.
- [31] L. Qin, X. Liang, H. Huang, C. K. Chui, R. C.-H. Yeow, and J. Zhu, "A versatile soft crawling robot with rapid locomotion," *Soft robotics*, 2019.
- [32] Z. Yang, L. Zhu, B. Li, S. Sun, Y. Chen, Y. Yan, Y. Liu, and X. Chen, "Mechanical design and analysis of a crawling locomotion enabled by a laminated beam," *Extreme Mechanics Letters*, vol. 8, pp. 88–95, 2016.
- [33] L. Zhu, Y. Cao, Y. Liu, Z. Yang, and X. Chen, "Architectures of soft robotic locomotion enabled by simple mechanical principles," *Soft matter*, vol. 13, no. 25, pp. 4441–4456, 2017.
- [34] U. Scarfogliero, C. Stefanini, and P. Dario, "Design and development of the long-jumping" grillo" mini robot," in *Proceedings 2007 IEEE International Conference on Robotics and Automation*. IEEE, 2007, pp. 467–472.
- [35] M. Kovac, M. Fuchs, A. Guignard, J.-C. Zufferey, and D. Floreano, "A miniature 7g jumping robot," in *Robotics and Automation, 2008. ICRA 2008. IEEE International Conference on*. IEEE, 2008, pp. 373–378.
- [36] C. S. Haines, M. D. Lima, N. Li, G. M. Spinks, J. Foroughi, J. D. Madden, S. H. Kim, S. Fang, M. J. De Andrade, F. Göktepe *et al.*, "Artificial muscles from fishing line and sewing thread," *science*, vol. 343, no. 6173, pp. 868–872, 2014.
- [37] S. Shian, K. Bertoldi, and D. R. Clarke, "Use of aligned fibers to enhance the performance of dielectric elastomer inchworm robots," in *Electroactive Polymer Actuators and Devices (EAPAD) 2015*, vol. 9430. International Society for Optics and Photonics, 2015, p. 94301P.
- [38] B. Goldberg, N. Doshi, K. Jayaram, J.-S. Koh, and R. J. Wood, "A high speed motion capture method and performance metrics for studying gaits on an insect-scale legged robot," in *2017 IEEE/RSJ International Conference on Intelligent Robots and Systems (IROS)*. IEEE, 2017, pp. 3964–3970.
- [39] Z. Zhakypov, K. Mori, K. Hosoda, and J. Paik, "Designing minimal and scalable insect-inspired multi-locomotion millirobots," *Nature*, 2019.
- [40] X. Ji, X. Liu, V. Cacucciolo, M. Imboden, Y. Civet, A. El Haitami, S. Cantin, Y. Perriard, and H. Shea, "An autonomous untethered fast soft robotic insect driven by low-voltage dielectric elastomer actuators," *Science Robotics*, vol. 4, no. 37, 2019.
- [41] R. M. Alexander, "Models and the scaling of energy costs for locomotion," *Journal of Experimental Biology*, vol. 208, no. 9, pp. 1645–1652, 2005.